

RESEARCH ARTICLE

Open Access

Structural characterization of a ribose-5-phosphate isomerase B from the pathogenic fungus *Coccidioides immitis*

Thomas E Edwards^{1,2*}, Ariel B Abramov^{1,3}, Eric R Smith^{1,2}, Ruth O Baydo^{1,2}, Jess T Leonard^{1,2}, David J Leibly^{1,4}, Kaitlin B Thompkins^{1,3}, Matthew C Clifton^{1,2}, Anna S Gardberg^{1,2}, Bart L Staker^{1,2}, Wesley C Van Voorhis^{1,4}, Peter J Myler^{1,3,5} and Lance J Stewart^{1,2}

Abstract

Background: Ribose-5-phosphate isomerase is an enzyme that catalyzes the interconversion of ribose-5-phosphate and ribulose-5-phosphate. This family of enzymes naturally occurs in two distinct classes, RpiA and RpiB, which play an important role in the pentose phosphate pathway and nucleotide and co-factor biogenesis.

Results: Although RpiB occurs predominantly in bacteria, here we report crystal structures of a putative RpiB from the pathogenic fungus *Coccidioides immitis*. A 1.9 Å resolution apo structure was solved by combined molecular replacement and single wavelength anomalous dispersion (SAD) phasing using a crystal soaked briefly in a solution containing a high concentration of iodide ions. RpiB from *C. immitis* contains modest sequence and high structural homology to other known RpiB structures. A 1.8 Å resolution phosphate-bound structure demonstrates phosphate recognition and charge stabilization by a single positively charged residue whereas other members of this family use up to five positively charged residues to contact the phosphate of ribose-5-phosphate. A 1.7 Å resolution structure was obtained in which the catalytic base of *C. immitis* RpiB, Cys76, appears to form a weakly covalent bond with the central carbon of malonic acid with a bond distance of 2.2 Å. This interaction may mimic that formed by the suicide inhibitor iodoacetic acid with RpiB.

Conclusion: The *C. immitis* RpiB contains the same fold and similar features as other members of this class of enzymes such as a highly reactive active site cysteine residue, but utilizes a divergent phosphate recognition strategy and may recognize a different substrate altogether.

Background

Ribose-5-phosphate isomerases catalyze the interconversion of ribulose-5-phosphate and ribose-5-phosphate as an important part of the pentose phosphate pathway [1]. Ribose-5-phosphate is used in nucleotide and co-factor biosynthesis. As with other isomerases, ribose-5-phosphate catalyzes this reaction at near equilibrium. Two types of ribose-5-phosphate isomerases exist, RpiA and RpiB, which share little structural homology and have distinct active sites and mechanisms of action [2]. Most organisms such as *Escherichia coli* contain both RpiA and RpiB, but other organisms contain only one class of

Rpi. In *E. coli*, a double *rpia/rpib* knockout exhibited severely impaired growth [3]. RpiB occurs almost exclusively in bacteria.

RpiB is a member of the LacAB_rpiB superfamily of proteins (PFAM PF02502). RpiB from different organisms may have different substrate specificities and several annotated RpiB enzymes act upon alloose-5-phosphate rather than or in addition to ribose-5-phosphate and are thus named AlsI. Indeed, one of the first crystal structures solved for a member of this family was the *E. coli* RpiB/AlsI [2]. Given the important cellular role of ribose-5-phosphate isomerases and that mammals only have RpiA, interest has been generated in RpiB enzymes as potential drug targets, especially in pathogenic organisms, many of which only have RpiB. *E. coli* RpiB inhibitors have been described [4] and

* Correspondence: tedwards@embios.com

¹Seattle Structural Genomics Center for Infectious Disease (SSGCID), USA
Full list of author information is available at the end of the article

inhibitor-bound crystal structures have been determined for RpiB from *Mycobacterium tuberculosis* [5] which causes tuberculosis and *Trypanosma cruzi* [6], the causative agent of trypanosomiasis.

Coccidioides immitis is a pathogenic fungus that causes coccidioidomycosis, also known as Valley Fever [7-9]. One gene (CIMG_07932) encodes a putative uncharacterized protein that contains high sequence homology with RpiB enzymes from closely related organisms. Specifically, the CIMG_07932 gene product contains 98% sequence identity to an Rpi from *C. posadasii*, 89% sequence identity to an Rpi from the non-pathogenic fungus *Uncinocarpus reesii*, and 78% sequence identity to an RpiB from *Paracoccidioides brasiliensis*. We have undertaken structural analysis of RpiB from *C. immitis* and present here crystal structures in apo and ligand bound forms.

Results and Discussion

Structure determination of *C. immitis* RpiB

Given that the *C. immitis* RpiB contains modest sequence identity to other structurally characterized RpiBs, we attempted to solve the crystal structure of *C. immitis* RpiB by iodide ion single wavelength anomalous dispersion (SAD) phasing [10,11], a strategy that has proven successful for structure determination of many SSGCID targets [12,13]. Attempts at phasing entirely with SAD resulted in poor quality experimental phases (FOM of 0.29 prior to density modification). Attempts to solve the structure by molecular replacement with other RpiBs such as that from *Clostridium thermocellum* [14] yielded clear rotation and translation solutions, yet poor refinement statistics (R of 0.39 and R_{free} 0.47). Addition of the MR solution to a SAD experiment has been shown to improve phase quality [15]. Therefore the partial molecular replacement solution was combined with the SAD phases and yielded a clearly interpretable electron density map (FOM 0.53 prior to density modification) into which Buccaneer [16] built both molecules in the asymmetric unit end-to-end in less than one minute (Table 1; Figure 1).

Interestingly, the active site contains electron density consistent with an oxidized cysteine residue (Cys76) in both protomers (Figure 1). Although the exact oxidation state of the cysteine residue was not determined, the electron density maps were most consistent with two conformations of the sulfenic state rather than sulfinic or sulfonic acid. The oxygen on Cys76 appears to adopt two different orientations contacting the backbone nitrogen and side chain hydroxyl of Thr78 in one orientation and the backbone nitrogens of Gly81 and Val82 in the other. The oxidized nature of Cys76 may imply that this residue, thought to be the catalytic base, is highly reactive. The high concentration solution of

sodium iodide used for phasing likely contains iodine, indicated by a light yellow color. Iodine is the most probable source for the oxidation of Cys76, which was not oxidized in the other two *C. immitis* RpiB structures (see below). Oxidation is unlikely to have occurred as a result of radiation damage since the data were collected in house under cryogenic temperatures. Oxidized cysteines have been observed previously in the presence of iodide ions [17,18] and also for other RpiB enzymes (PDB entries 1O1X [19] and 3C5Y, no primary citation) determined in the absence of iodide.

Comparison with other ribose-5-phosphate isomerases

The *C. immitis* RpiB contains ~20-38% sequence identity with other structurally characterized RpiB enzymes, although fewer than 10 amino acids are completely conserved across these sequences (Figure 2). The overall structure of the *C. immitis* putative RpiB is quite similar to other structurally characterized RpiB enzymes from bacterial as well as eukaryotic organisms (Table 2). In addition to the conserved overall fold, certain other RpiB features are present in the *C. immitis* RpiB structure such as the highly conserved cis-peptide at residue Gly43.

The *C. immitis* RpiB contains the canonical open (α,β) Rossmann fold, a common fold for proteins that bind nucleotides or nucleotide-like molecules [20]. As determined by the Protein Interfaces, Surfaces and Assemblies (PISA) server [21], the quaternary structure appears to be dimeric (Figure 1) with 7408 Å² of buried surface (12,690 Å² of surface area for the dimer). However, based on the structure, PISA also predicts a tetrameric structure (generated by crystal symmetry) in which 17,610 Å² of surface area is buried (22,730 Å² of surface area for the tetramer). The tetrameric structure of *C. immitis* RpiB is most likely a dimer of dimers with one strong dimer and the secondary weaker dimer interaction that makes the tetramer. This quaternary structure is consistent with the two ligand bound *C. immitis* RpiB described below in a different crystal form, and with previous X-ray structural characterization of RpiB, such as that from *E. coli* [2]. Dynamic light scattering (DLS) experiments indicated a monodisperse protein with an approximate molecular weight of 80 kDa which is consistent with a tetramer in solution. DLS measurement on *E. coli* RpiB also indicated a tetramer in solution [2]. Thermofluor analysis indicated a stable protein with a melting temperature of 52°C. The melting temperature was unaffected by the presence of ribose-5-phosphate, ribose-5-phosphate with MnCl₂, or iodoacetate.

C. immitis RpiB substrate recognition

Structures of RpiB from other organisms have been obtained in the presence of ribose-5-phosphate or

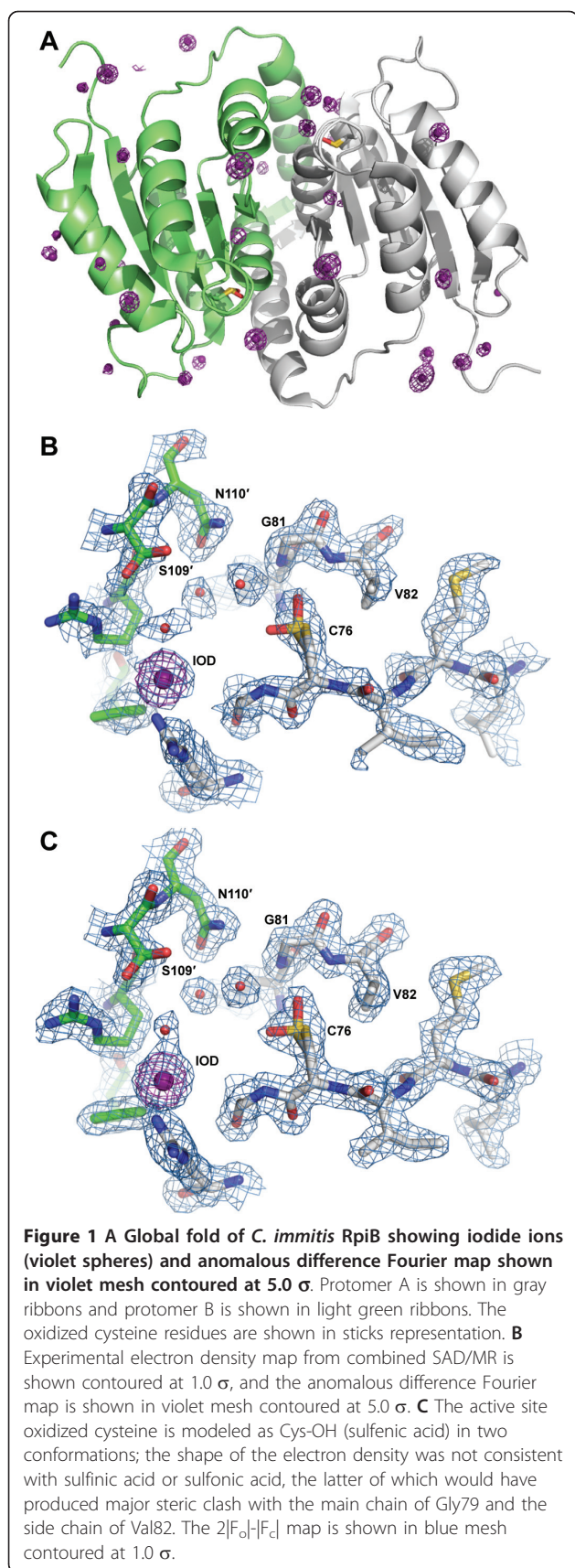
Table 1 Data collection, phasing and refinement statistics

	Iodide	Phosphate	Malonic acid
<i>Data reduction</i>			
Space group	C2	F222	F222
Unit-cell parameters	$a = 103.2 \text{ \AA}$, $b = 49.9 \text{ \AA}$, $c = 62.0 \text{ \AA}$, $\beta = 108.6^\circ$	$a = 77.7 \text{ \AA}$, $b = 85.2 \text{ \AA}$, $c = 96.3 \text{ \AA}$	$a = 77.5 \text{ \AA}$, $b = 84.4 \text{ \AA}$, $c = 96.2 \text{ \AA}$
Resolution range (\AA)	50-1.9 (1.95-1.90)	50-1.8 (1.85-1.80)	50-1.7 (1.74-1.70)
Unique reflections	23,513 (1520)	14,967 (1088)	16,561 (1028)
R_{merge}	0.043 (0.286)	0.123 (0.397)	0.044 (0.256)
Mean $I/\sigma(I)$	13.9 (2.9)	17.5 (3.0)	34.7 (6.6)
Completeness	98.9% (87.5%)	99.8% (98.7%)	94.5% (80.2%)
Multiplicity	5.8 (2.9)	6.9 (3.9)	9.6 (5.3)
<i>Phasing</i>			
Anomalous Correlation	58% (8%)		
SigAno	1.53 (0.81)		
Iodide Sites	21		
FOM (Phaser EP)	0.53		
<i>Refinement</i>			
R_{cryst}	0.166 (0.185)	0.150 (0.212)	0.144 (0.156)
R_{free}	0.205 (0.242)	0.176 (0.270)	0.175 (0.189)
RMSD bonds (\AA)	0.015	0.015	0.012
RMSD angles ($^\circ$)	1.364	1.288	1.323
Protein Atoms	2415	1198	1210
Waters	213	173	169
Iodide Ions	29	0	0
Mean B -factor (\AA^2)	18.3	13.2	13.7
Reflections	22,275 (1434)	14,170 (1031)	15,677 (968)
R_{free} Reflections	1205	752	832
<i>Validation</i>			
Ramachandran favored	100%	100%	98.7%
Ramachandran outliers	0%	0%	0%
Molprobability score [35]	1.42 (97 th percentile)	0.98 (100 th)	1.32 (97 th)
PDB ID	3QD5	3SDW	3SGW

$R_{\text{free}} = \sum_n |F_{\text{obs}}| - |F_{\text{calc}}| / \sum_n |F_{\text{obs}}|$. Values in parenthesis indicate the values for the highest of twenty resolution shells
 R_{free} was calculated using 5% of the reflections omitted from the refinement [31].

inhibitors. Comparison of the active site in multiple sequence alignments showed that several residues involved in recognition of the phosphate moiety of ribose-5-phosphate or ribulose-5-phosphate are not conserved in *C. immitis* RpiB (Figure 2). While other organisms use up to five positively charged residues to recognize the phosphate moiety, only one of these residues is positively charged (Lys148) in *C. immitis*. Several other residues are small polar residues such as Ser109 and Ser145. Residue 17 is typically a histidine or asparagine, but is surprisingly a negatively charged aspartic acid residue in *C. immitis*. Because of the decreased size of several residues and the presence of Asp17, we speculated that the *C. immitis* RpiB may utilize a cation to facilitate recognition of ribose-5-phosphate. RpiB

enzymes from other organisms typically recognize ribose-5-phosphate with a low affinity of $K_m \sim 1\text{-}5 \text{ mM}$ [2,22]. Therefore, we performed co-crystallization experiments in the presence of 20 mM ribose-5-phosphate or 20 mM ribose-5-phosphate with 12 mM MnCl_2 , which are in excess of the protein ($\sim 3.3 \text{ mM}$). We obtained a 1.8 \AA resolution data set (Table 1) from *C. immitis* RpiB co-crystallized in the presence of 20 mM ribose-5-phosphate and 12 mM MnCl_2 . Despite the presence of 20 mM substrate, we only observed substantial electron density for phosphate bound in the active site, which presumably came from the 0.1 M SPG buffer (succinic acid, phosphate, glycine) buffer at pH 5.0 (Figure 3). Therefore, it appears that under the conditions of the crystallization experiment, phosphate



outcompeted ribose-5-phosphate for binding to the active site. Addition electron density extends from one of the oxygens of the phosphate. The crystal may contain a mixture of phosphate and ribose-5-phosphate, which could be modeled into the active site without significant steric clash. Refinement of ribose-5-phosphate alone or at 0.5 occupancy with phosphate as the other 0.5 occupancy resulted in negative density in the $|F_o|-|F_c|$ electron density map and high crystallographic B -factors for ribose-5-phosphate. Therefore, the final model contains only phosphate. Phosphate is recognized by Ser109, Ser145 and Lys148 of the active site. Some of the negative charge may be stabilized via charge relay from Ser109 to Arg105. In other organisms, Arg105 is a leucine or methionine (Figure 2). The positioning of the phosphate moiety is slightly different than that observed in other structures, such as that of *T. cruzi* RpiB bound to the competitive inhibitor 4-deoxy-4-phospho-D-erythronhydroxamic acid [6] (Figure 4).

Given the substantial differences in the active site of the *C. immitis* RpiB in comparison with other structurally and functionally characterized RpiB enzymes, it is possible that the *C. immitis* enzyme utilizes a substrate different than ribose-5-phosphate/ribulose-5-phosphate. In addition to the single positively charged residue that interacts with the phosphate, the highly conserved histidine involved in ring opening in the catalytic mechanism (His102" in *C. thermocellum* [14]) has been replaced with Ser109" in the *C. immitis* structure (Figure 4). Given the position of the phosphate in the *C. immitis* structure, we suspect that this enzyme may isomerize shorter chain substrates, although confirmation of substrate activity will require further structural and biochemical characterization. Furthermore, *C. immitis* contains another gene (CIMG_09662) that encodes a putative uncharacterized protein which contains 99% sequence identity to RpiA from *C. posadasii* (gene CPC735_023760). Therefore, this essential function of the pentose phosphate pathway may be accomplished by RpiA, allowing RpiB to have evolved with an altered substrate specificity.

C. immitis RpiB covalent inhibition

The catalytic cysteine residue of RpiB is known to be reactive toward iodoacetate [2,23], although no crystal structure has been determined for an RpiB covalently bound to iodoacetate. Attempts at co-crystallization after incubation with 10 mM iodoacetamide did not yield diffraction quality crystals. However, a 1.7 Å resolution data set was obtained from a crystal grown from MIB buffer (malonic acid, imidazole, boric acid) at pH 5.0 which contained clear evidence for malonic acid tightly bound off Cys76 (Figure 5). The malonic acid refines with a C2-S distance of 2.2 Å, which is longer

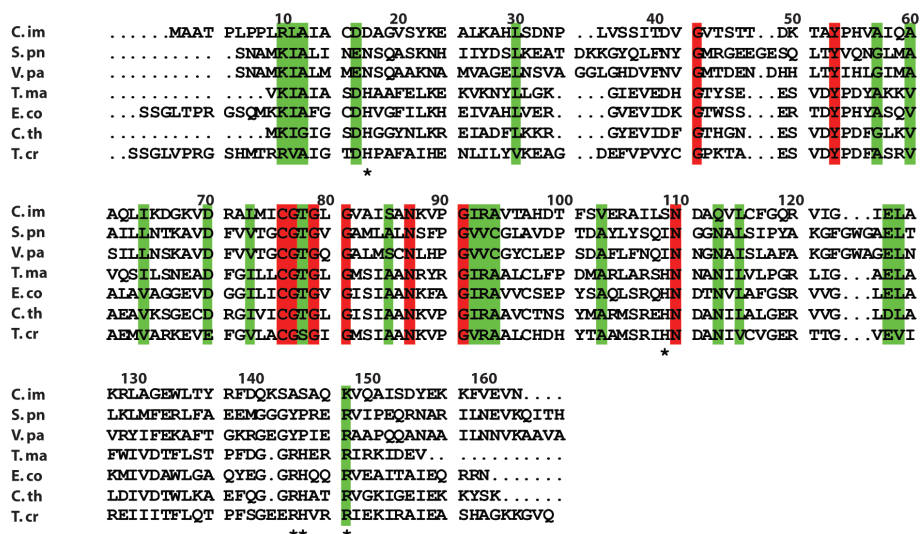


Figure 2 Multiple sequence alignment of RpiB crystal structures from different organisms. *C. immitis* is from the current study (PDB ID 3QD5). *S. pu* is *Streptococcus pneumoniae* (2PPW, no primary citation), *V. pa* is *Vibrio parahaemolyticus* (3ONO, no primary citation), *T. ma* is *Thermotoga maritima* (PDB ID 1O1X) [19], *E. co* is *E. coli* (1NN4) [2], *C. th* is *Clostridium thermocellum* (3HEE) [14], *T. cr* is *Trypanosoma cruzi* (3K8C) [6]. *Mycobacterium tuberculosis* contains different active site residues and utilizes a variant catalytic mechanism [5,22], and thus the sequence is not shown in the alignment. Residues marked with an * are involved in recognition of the phosphate moiety of ribose-5-phosphate. Numbering is based on the *C. immitis* sequence.

than that expected for a covalent C-S bond (1.8 Å), but significantly shorter than that expected for van der Waals interactions (>3.3 Å); malonic acid was built into the omit $|F_o| - |F_c|$ density and allowed to refine freely in REFMAC5 [24]. Therefore, this structure may reflect the formation of a distorted (long) covalent bond between malonic acid and Cys76. We do not know of a reasonable mechanism for the formation of such a covalent bond between malonic acid and Cys76, which rather seems counterintuitive.

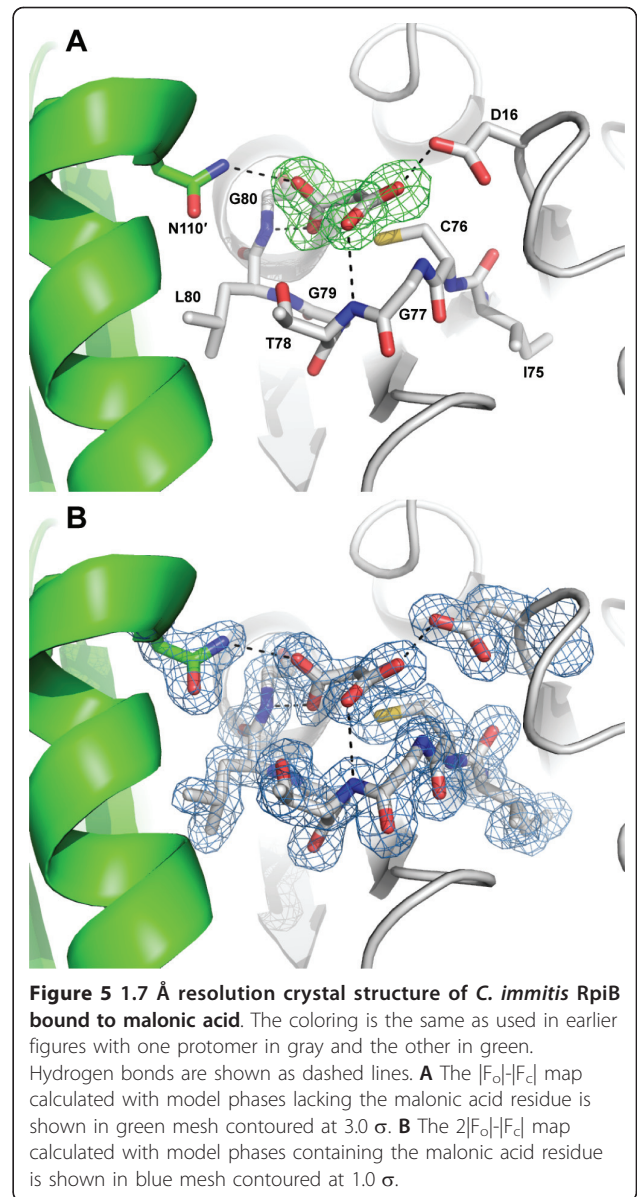
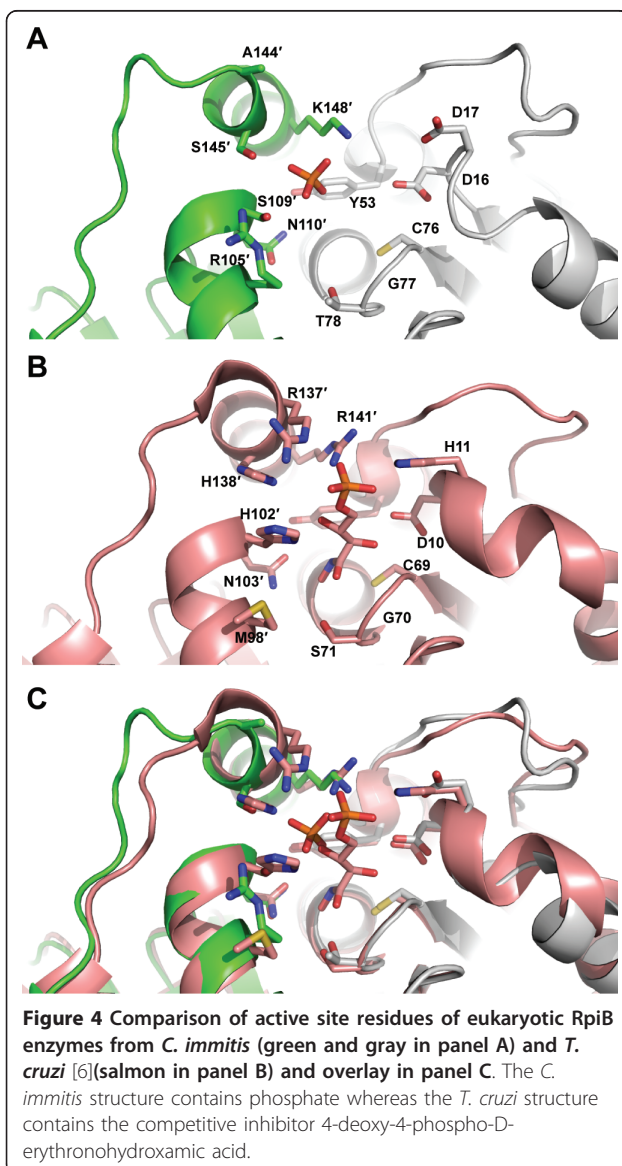
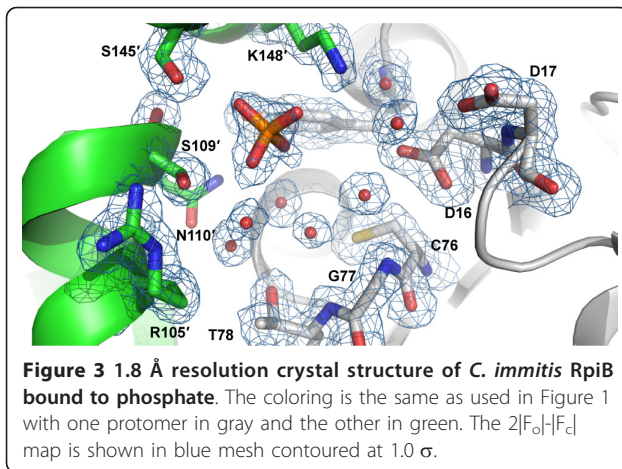
The chemical reaction of Cys76 with iodoacetate is expected to form a Cys-CH₂COOH adduct. The

conformation of either of the carboxylates of malonic acid may be reflective of the carboxylate of the covalent adduct formed with iodoacetate. One of the carboxylates of malonic acid forms hydrogen bonds with the backbone amides of Thr78 (conserved as a serine or threonine, 3.0 Å) and the universally conserved Gly77 (2.9 Å) as well as the side chain of the universally conserved Asp16 (2.6 Å). The hydrogen bond with Asp16 is unlikely to occur at neutral pH where both carboxylates are expected to be deprotonated and negatively charged. In contrast, the interaction is well ordered in the pH 5.0 crystal. Given an approximate pKa of ~4.8, at pH 5.0

Table 2 Comparison of the global structure of *C. immitis* RpiB with RpiB enzymes from other organisms

Organism	Reference PDB	Similar Cα atoms	R.m.s.d. (Å)	Identity (%)
Bacteria				
<i>Clostridium thermocellum</i>	3HEE [14]	148	1.17	34
<i>Escherichia coli</i>	1NN4 [2]	143	1.10	38
<i>Mycobacterium tuberculosis</i>	2VVO [5,22]	141	1.18	26
<i>Novosphingobium aromaticivorans</i>	3CSY	149	1.97	<20
<i>Streptococcus pneumoniae</i>	2PPW	146	1.91	<20
<i>Thermotoga maritima</i>	1O1X [19]	143	1.24	33
<i>Vibrio parahaemolyticus</i>	3ONO	149	1.86	<20
Eukaryotes				
<i>Giardia lamblia</i>	3SSP	125	1.06	28
<i>Trypanosoma cruzi</i>	3K8C [6]	148	1.40	29

Superposition calculations were done in CCP4 using the program Superposition and the secondary structure matching setting. The number of similar Cα atoms (residues) is reported. For PDB entries 3CSY (UCSG), 2PPW (Wu, R. et al.), 3ONO (Kim, Y. et al.) and 3SSP (Edwards, T.E. et al.) no primary citation has been reported.



about half of the carboxylates should be protonated. The second malonic acid carboxylate forms hydrogen bonding interactions with the backbone amide nitrogen of the universally conserved Gly81 (2.5 Å) and with the side chain of the universally conserved Asn110' of the other protomer of the obligate dimeric enzyme (3.0 Å). The interactions of this carboxylate with RpiB may reflect the interactions formed by the iodoacetate covalent adduct. There is a chloride ion in the active site 3.7 Å away from the malonic acid and near Arg105' and Arg120, although this anion is ill-suited to mimic the iodide ion leaving group of iodoacetate because it is on the opposite side of the carboxylate relative to Cys76. An iodide ion resides in the same place as this chloride ion

in both protomers of the asymmetric unit in the iodide-phased structure.

Conclusions

Here we present crystal structures of RpiB from the pathogenic fungus *C. immitis*, which together with the structures from *T. cruzi* [6] and *G. lamblia* (Edwards, T. E. et al., unpublished) are the only eukaryotic RpiB crystal structures currently available. These structures reveal the presence of a highly reactive cysteine residue in the active site, thought to be the catalytic base in the isomerase reaction and provide insight into a possible structural mechanism for the inhibition of RpiB by iodoacetate. Furthermore, these structures reveal the basis for phosphate recognition by a single positively charged residue and may indicate that this *C. immitis* has altered substrate specificity.

Methods

Cloning, expression, and purification

The 163-residue *Coccidioides immitis* putative uncharacterized protein (*C. immitis* RpiB, UniProt ID: P0CL19, formerly Q1DP31; Gene CIMG_07932, targetDB ID: CoimA.00584.a, E. C. 5.3.1.6) was amplified from genomic DNA and cloned into an expression vector (pAVA0421) encoding an N-terminal histidine affinity tag followed by the human rhinovirus 3C protease cleavage sequence using ligation independent cloning [25]. The full length expressed protein contains the tag sequence MAHHHHHHMGTLEAQTQGP GS followed by the 163-residue *C. immitis* RpiB. The plasmid is available through the BEI repository (NR-28451). The plasmid was transformed into *E. coli* BL21 (DE3) R3 Rosetta cells. Starter cultures of LB broth with appropriate antibiotics were grown for ~18 hours at 37°C. Protein was expressed in a LEX bioreactor in ZYP-5052 auto-induction media [26] in the presence of antibiotics in 2 liters of sterilized auto-induction media inoculated with the overnight starter culture. After 24 hours at 25°C the temperature was reduced to 15°C for an additional 60 hours. The sample was centrifuged at 4000 × g for 20 minutes at 4°C. Cell paste was flash frozen in liquid nitrogen and stored at -80°C. The frozen cells were re-suspended in 20 mM HEPES pH 7.0, 300 mM NaCl, 5% w/v glycerol, 0.5% w/v CHAPS, 30 mM imidazole, 10 mM MgCl₂, 1 mM TCEP, 250 µg/ml AEBSEF, 200 µl of lysozyme (100 mg/mL), 5 tablets of Roche protease inhibitor tablets, and 280 µl of β-mercaptoethanol at 4°C. Lysis was achieved by sonication, followed by incubation with Benzonase (20 µL of 25 unit/µL). Insoluble proteins and other cellular components were removed by centrifugation at 10,000 rpm for 60 minutes at 4°C. The supernatant was filtered using a low-protein binding 0.45 µm sterile filter. The soluble fraction was

then loaded onto a Ni-NTA His-Trap FF 5 ml column (GE Healthcare). The column was washed with 20 column volumes of wash buffer (20 mM HEPES pH 7.0, 300 mM NaCl, 5% w/v glycerol, 30 mM imidazole, and 1 mM TCEP). The bound protein was eluted with 7 column volumes of elution buffer (20 mM HEPES pH 7.0, 300 mM NaCl, 5% w/v glycerol, 1 mM TCEP, and 500 mM imidazole). The collected protein was loaded onto a Hiload 26/60 Superdex 75 prep grade column (GE Healthcare) equilibrated in SEC buffer (20 mM HEPES pH 7.0, 300 mM NaCl, 5% v/v glycerol, and 1 mM TCEP). The protein eluted off the SEC column in a split peak, which was pooled into two samples and concentrated to 82 mg/mL for the first peak sample and 128 mg/mL for the second peak sample. Both samples were shown by sodium dodecyl sulfate polyacrylamide gel electrophoresis to be >95% pure and contain a protein of the expected molecular weight. Therefore, the two samples may reflect different oligomeric states of the same protein in solution. The sample from the first peak resulted in the crystal structures, whereas the sample from the second peak yielded crystals which did not diffract to better than 3 Å resolution. The purified protein samples were stored at -80°C. Dynamic light scattering (DLS) was performed at 8 mg/mL in SEC buffer on a Malvern Instruments Nano series Zetasizer. Thermofluor experiments were performed in SEC buffer at 2 and 4 mg/mL as described [27].

Crystallization and structure determination

Crystallization trials were set up according to a crystallization approach [28] using the JCSG+ and PACT sparse matrix screens from Emerald BioSystems. Protein drops (0.4 µL at 82 mg/mL) were diluted with an equal volume of precipitant and equilibrated against 80 µL of precipitant in 96-well sitting drop vapor diffusion format using Compact Junior plates from Emerald BioSystems. A crystal grown from the JCSG+ screen condition B9 (0.1 M Na citrate pH 5.0, 20% w/v PEG 6000) was soaked into a solution containing 0.1 M Na citrate pH 5.0, 20% w/v PEG 6000, 22% v/v ethylene glycol, and 0.7 M NaI for 1 minute, then vitrified in liquid nitrogen. A data set (Table 1) was collected at 100 K under a stream of liquid nitrogen using a Rigaku FR-E+ SuperBright Cu K α rotating anode X-ray generator with VariMax optics and a Saturn 944+ CCD detector. Data parameters include 360 images, $\Delta\phi = 1^\circ$, $2\theta = 5^\circ$, 20 s exposure times, and a detector distance of 50 mm. Data were reduced with XDS [29]. The structure was solved by combined molecular replacement and iodide ion SAD phasing. First, molecular replacement was performed using the protein model from protomer A of *Clostridium thermocellum* crystal structure (PDB ID 3HEE, [14]) as a search model in Phaser [30] from the CCP4

suite [31]. Separately, twenty-one anomalous sites were identified using *phenix.hyss* [32]. Phases calculated from SAD were combined with the MR solution in Phaser EP [30]. After density improvement in parrot [33], the model was initially built using Buccaneer [16] using the default parameters for both programs and Hendrickson Lattman coefficients and R_{free} rather than Phi/FOM. Another crystal of *C. immitis* RpiB was grown at 66 mg/mL in the presence of 20 mM ribose-5-phosphate and 12 mM $MnCl_2$ in the PACT screen condition A2 (0.1 M SPG buffer pH 5.0, 25% w/v PEG 1500). The crystal was cryo-protected in a solution containing 20 mM ribose-5-phosphate, 12 mM $MnCl_2$, 0.1 M SPG buffer pH 4.0, 30% w/v PEG 1500 and 20% v/v ethylene glycol and vitrified. A data set was collected as described above for the iodide crystal with the exception of $2\theta = 10^\circ$, 340 images and 30 s exposure times. The phosphate bound structure was solved by molecular replacement in Phaser [30] using the protein-only model of the iodide phased structure. A third crystal of *C. immitis* RpiB was grown at 66 mg/mL in the presence of 20 mM ribose-5-phosphate and 12 mM $MnCl_2$ in the PACT screen condition B2 (0.1 M MIB buffer pH 5.0, 25% w/v PEG 1500). The crystal was cryo-protected in a solution containing 20 mM ribose-5-phosphate, 12 mM $MnCl_2$, 0.1 M MIB buffer pH 4.0, 30% w/v PEG 1500 and 20% v/v ethylene glycol and vitrified. A data set was collected as described above for the iodide crystal with the exception of $2\theta = 10^\circ$, 360 images and 6 s exposure times. This malonic acid bound structure was solved using the protein model from the phosphate-bound structure. The final models (Table 1) were obtained after numerous rounds of refinement in REFMAC5 [24] and manual re-building in COOT [34]. NCS averaging was not used due to the high resolution of each structure (sub 2 Å). Both $2|F_o| - |F_c|$ and $|F_o| - |F_c|$ electron density maps were used in model building. TLS refinement was used with one group per chain. Water molecules were built that were within hydrogen bonding distance to the protein (~3.2 Å) and showed electron density above 1.1 σ in the final $2|F_o| - |F_c|$ electron density map. Structures were assessed for correctness and validated using Molprobity [35]. All diffraction images are freely available (http://www.csgid.org/csgid/pages/diffraction_images).

Acknowledgements and Funding

The authors thank the whole SSGCID team. This research was funded under Federal Contract Number HHSN272200700057C from the National Institute of Allergy and Infectious Diseases, National Institutes of Health, Department of Health and Human Services.

Author details

¹Seattle Structural Genomics Center for Infectious Disease (SSGCID), USA. ²Emerald BioStructures, 7869 NE Day Road West, Bainbridge Island, WA, 98110, USA. ³Seattle Biomedical Research Institute, 307 Westlake Avenue North, Suite 500, Seattle, WA 98109, USA. ⁴School of Medicine, University of

Washington, 1959 N.E. Pacific Avenue, MS 356423, Seattle, WA 98195-7185, USA. ⁵Departments of Global Health and Medical Education & Biomedical Informatics, University of Washington, Box 357230, Seattle, WA 98195, USA.

Authors' contributions

TEE collected two of the data sets, solved all three structures, analyzed the data and wrote the paper. ABA purified the protein. ERS performed DLS measurements. ROB performed thermofluor analysis. JTL collected one data set. DJL performed large scale expression and KBT performed lysis. MCC verified two structures, and ASG verified the other. BLS is the SSGCID site manager. WCV is an SSGCID Co-PI. PJM is the SSGCID PI. LJS is an SSGCID Co-PI. All authors read and approved the final manuscript.

Received: 1 July 2011 Accepted: 13 October 2011

Published: 13 October 2011

References

1. Wamelink MM, Struys EA, Jakobs C: The biochemistry, metabolism and inherited defects of the pentose phosphate pathway: a review. *J Inher Metab Dis* 2008, **31**(6):703-717.
2. Zhang RG, Andersson CE, Skarina T, Evdokimova E, Edwards AM, Joachimiak A, Savchenko A, Mowbray SL: The 2.2 Å resolution structure of RpiB/AlsB from *Escherichia coli* illustrates a new approach to the ribose-5-phosphate isomerase reaction. *J Mol Biol* 2003, **332**(5):1083-1094.
3. Sorensen KI, Hove-Jensen B: Ribose catabolism of *Escherichia coli*: characterization of the rpiB gene encoding ribose phosphate isomerase B and of the rpiR gene, which is involved in regulation of rpiB expression. *J Bacteriol* 1996, **178**(4):1003-1011.
4. Mariano S, Roos AK, Kowalinski E, Salmon L, Mowbray SL: Competitive inhibitors of type B ribose 5-phosphate isomerases: design, synthesis and kinetic evaluation of new D-allose and D-allulose 6-phosphate derivatives. *Carbohydr Res* 2009, **344**(7):869-880.
5. Roos AK, Mariano S, Kowalinski E, Salmon L, Mowbray SL: D-ribose-5-phosphate isomerase B from *Escherichia coli* is also a functional D-allose-6-phosphate isomerase, while the *Mycobacterium tuberculosis* enzyme is not. *J Mol Biol* 2008, **382**(3):667-679.
6. Stern AL, Naworyta A, Cazzulo JJ, Mowbray SL: Structures of type B ribose 5-phosphate isomerase from *Trypanosoma cruzi* shed light on the determinants of sugar specificity in the structural family. *FEBS J* 2011, **278**(5):793-808.
7. Deus Filho A: Chapter 2: coccidioidomycosis. *J Bras Pneumol* 2009, **35**(9):920-930.
8. Hector RF, Laniado-Laborin R: Coccidioidomycosis—a fungal disease of the Americas. *PLoS Med* 2005, **2**(1):e2.
9. Sharpton TJ, Stajich JE, Rounsley SD, Gardner MJ, Wortman JR, Jordar VS, Maiti R, Kodira CD, Neafsey DE, Zeng Q, et al: Comparative genomic analyses of the human fungal pathogens *Coccidioides* and their relatives. *Genome Res* 2009, **19**(10):1722-1731.
10. Dauter M, Dauter Z: Phase determination using halide ions. *Methods Mol Biol* 2007, **364**:149-158.
11. Dauter Z, Dauter M, Rajashankar KR: Novel approach to phasing proteins: derivatization by short cryo-soaking with halides. *Acta Crystallogr D Biol Crystallogr* 2000, **56**(Pt 2):232-237.
12. Abendroth J, Gardberg AS, Robinson JI, Christensen JS, Staker BL, Myler PJ, Stewart LJ, Edwards TE: SAD phasing using iodide ions in a high-throughput structural genomics environment. *J Struct Funct Genomics* 2011, **12**(2):83-95.
13. Edwards TE, Phan I, Abendroth J, Dieterich SH, Masoudi A, Guo W, Hewitt SN, Kelley A, Leibly D, Brittnacher MJ, et al: Structure of a *Burkholderia pseudomallei* trimeric autotransporter adhesin head. *PLoS One* 2010, **5**(9):e12803.
14. Jung J, Kim JK, Yeom SJ, Ahn YJ, Oh DK, Kang LW: Crystal structure of *Clostridium thermocellum* ribose-5-phosphate isomerase B reveals properties critical for fast enzyme kinetics. *Appl Microbiol Biotechnol* 2011, **90**(2):517-527.
15. Roversi P, Johnson S, Lea SM: With phases: how two wrongs can sometimes make a right. *Acta Crystallogr D Biol Crystallogr* 2010, **66**(Pt 4):420-425.
16. Cowtan K: The Buccaneer software for automated model building. 1. Tracing protein chains. *Acta Crystallogr D Biol Crystallogr* 2006, **62**(Pt 9):1002-1011.

17. Galalaldein A, Strange RW, Whitson LJ, Antonyuk SV, Narayana N, Taylor AB, Schuermann JP, Holloway SP, Hasnain SS, Hart PJ: **Structural and biophysical properties of metal-free pathogenic SOD1 mutants A4V and G93A.** *Arch Biochem Biophys* 2009, **492**(1-2):40-47.
18. Pauwels K, Lustig A, Wyns L, Tommassen J, Savvides SN, Van Gelder P: **Structure of a membrane-based steric chaperone in complex with its lipase substrate.** *Nat Struct Mol Biol* 2006, **13**(4):374-375.
19. Xu Q, Schwarzenbacher R, McMullan D, von Delft F, Brinen LS, Canaves JM, Dai X, Deacon AM, Elsliger MA, Eshagi S, *et al*: **Crystal structure of a ribose-5-phosphate isomerase RpiB (TM1080) from *Thermotoga maritima* at 1.90 Å resolution.** *Proteins* 2004, **56**(1):171-175.
20. Rossmann MG, Moras D, Olsen KW: **Chemical and biological evolution of nucleotide-binding protein.** *Nature* 1974, **250**(463):194-199.
21. Krissinel E, Henrick K: **Inference of macromolecular assemblies from crystalline state.** *J Mol Biol* 2007, **372**(3):774-797.
22. Roos AK, Andersson CE, Bergfors T, Jacobsson M, Karlen A, Unge T, Jones TA, Mowbray SL: **Mycobacterium tuberculosis ribose-5-phosphate isomerase has a known fold, but a novel active site.** *J Mol Biol* 2004, **335**(3):799-809.
23. Essenberg MK, Cooper RA: **Two ribose-5-phosphate isomerases from *Escherichia coli* K12: partial characterisation of the enzymes and consideration of their possible physiological roles.** *Eur J Biochem* 1975, **55**(2):323-332.
24. Murshudov GN, Vagin AA, Dodson EJ: **Refinement of macromolecular structures by the maximum-likelihood method.** *Acta Crystallogr D Biol Crystallogr* 1997, **53**(Pt 3):240-255.
25. Aslanidis C, de Jong PJ: **Ligation-independent cloning of PCR products (LIC-PCR).** *Nucleic Acids Res* 1990, **18**(20):6069-6074.
26. Studier FW: **Protein production by auto-induction in high density shaking cultures.** *Protein Expr Purif* 2005, **41**(1):207-234.
27. Crowther GJ, He P, Rodenbough PP, Thomas AP, Kovzun KV, Leibly DJ, Bhandari J, Castaneda LJ, Hol WG, Gelb MH, *et al*: **Use of thermal melt curves to assess the quality of enzyme preparations.** *Anal Biochem* 2010, **399**(2):268-275.
28. Newman J, Egan D, Walter TS, Meged R, Berry I, Ben Jelloul M, Sussman JL, Stuart DI, Perrakis A: **Towards rationalization of crystallization screening for small- to medium-sized academic laboratories: the PACT/JCSG+ strategy.** *Acta Crystallogr D Biol Crystallogr* 2005, **61**(Pt 10):1426-1431.
29. Kabsch W: **Xds.** *Acta Crystallogr D Biol Crystallogr* 2010, **66**(Pt 2):125-132.
30. McCoy AJ, Grosse-Kunstleve RW, Adams PD, Winn MD, Storoni LC, Read RJ: **Phaser crystallographic software.** *J Appl Crystallogr* 2007, **40**(Pt 4):658-674.
31. **The CCP4 suite: programs for protein crystallography.** *Acta Crystallogr D Biol Crystallogr* 1994, **50**(Pt 5):760-763.
32. Adams PD, Afonine PV, Bunkoczi G, Chen VB, Davis IW, Echols N, Headd JJ, Hung LW, Kapral GJ, Grosse-Kunstleve RW, *et al*: **PHENIX: a comprehensive Python-based system for macromolecular structure solution.** *Acta Crystallogr D Biol Crystallogr* 2010, **66**(Pt 2):213-221.
33. Cowtan K: **Recent developments in classical density modification.** *Acta Crystallogr D Biol Crystallogr* 2010, **66**(Pt 4):470-478.
34. Emsley P, Cowtan K: **Coot: model-building tools for molecular graphics.** *Acta Crystallogr D Biol Crystallogr* 2004, **60**(Pt 12 Pt 1):2126-2132.
35. Chen VB, Arendall WB, Headd JJ, Keedy DA, Immormino RM, Kapral GJ, Murray LW, Richardson JS, Richardson DC: **MolProbity: all-atom structure validation for macromolecular crystallography.** *Acta Crystallogr D Biol Crystallogr* 2010, **66**(Pt 1):12-21.

doi:10.1186/1472-6807-11-39

Cite this article as: Edwards *et al.*: Structural characterization of a ribose-5-phosphate isomerase B from the pathogenic fungus *Coccidioides immitis*. *BMC Structural Biology* 2011 11:39.

Submit your next manuscript to BioMed Central and take full advantage of:

- Convenient online submission
- Thorough peer review
- No space constraints or color figure charges
- Immediate publication on acceptance
- Inclusion in PubMed, CAS, Scopus and Google Scholar
- Research which is freely available for redistribution

Submit your manuscript at
www.biomedcentral.com/submit

